Frontiers in Bioscience Landmark

Front. Biosci. (Landmark Ed) **2023**; 28(2): 23
https://doi.org/10.31083/j.fbl2802023

Original Research

Protective Effect of *Ganoderma lucidum* Spore Powder on Acute Liver Injury in Mice and its Regulation of Gut Microbiota

Yue Leng[1], Fang Wang[1], Changbao Chen[1], Xilin Wan[1], Xinyang Li[1], Huan Wang[1,*], Shumin Wang[1,*]

[1]Department of Ginseng Scientific Research Institute, Changchun University of Chinese Medicine, 130117 Changchun, Jilin, China
*Correspondence: wanghuanmyco@163.com (Huan Wang); wangsm@ccucm.edu.cn (Shumin Wang)

Academic Editor: Ru Chen
Submitted: 26 October 2022 Revised: 6 December 2022 Accepted: 9 December 2022 Published: 2 February 2023

Abstract

Background: *Ganoderma lucidum* spore powder (GLSP) has abundant pharmacological activities. However, the difference in the hepatoprotective function of sporoderm-broken and sporoderm-unbroken Ganoderma spore powder has not been studied. This study is the first to investigate the effects of both sporoderm-damaged and sporoderm-intact GLSP on the improvement of acute alcoholic liver injury in mice and gut microbiota of mice. **Methods**: Serum aspartate aminotransferase (AST) and alanine aminotransferase (ALT) levels and interleukin 1β (IL-1β), interleukin 18 (IL-18), and tumor necrosis factor-α (TNF-α) levels in liver tissues from mice in each group were detected by enzyme-linked immunosorbent assay (ELISA) kits, and histological analysis of liver tissue sections was performed to evaluate the liver-protecting effects of both sporoderm-broken and sporoderm-unbroken GLSP. Additionally, 16S rDNA sequencing of feces from the bowels of mice was performed to compare the regulatory effects of both sporoderm-broken and sporoderm-unbroken GLSP on the gut microbiota of mice. **Results**: Compared with those in the 50% ethanol model group (MG), sporoderm-broken GLSP significantly reduced serum AST and ALT levels ($p < 0.0001$) and the release of the inflammatory factors, including IL-1β, IL-18, and TNF-α ($p < 0.0001$), and effectively improved the pathological state of liver cells; sporoderm-unbroken GLSP significantly reduced the ALT content ($p = 0.0002$) and the release of the inflammatory factors, including IL-1β ($p < 0.0001$), IL-18 ($p = 0.0018$), and TNF-α ($p = 0.0005$), and reduced the serum AST content, but the reduction was not significant; compared with the gut microbiota of the MG, sporoderm-broken GLSP reduced the levels of *Verrucomicrobia* and *Escherichia_Shigella*, increased the relative abundance of beneficial bacteria such as *Bacteroidetes*, and decreased the abundance levels of harmful bacteria, such as *Proteobacteria* and *Candidatus_Saccharibacteria*; sporoderm-unbroken GLSP could reduce the abundance levels of harmful bacteria, such as *Verrucomicrobia* and *Candidatus_Saccharibacteria*; and GLSP treatment alleviates the downregulation of the levels of translation, ribosome structure and biogenesis, and lipid transport and metabolism in liver-injured mice; **Conclusions**: GLSP can alleviate the imbalance of gut microbiota and improve liver injury, and the effect of sporoderm-broken GLSP is better.

Keywords: sporoderm-broken *Ganoderma lucidum* spore powder; gut microbiota; alcoholic liver disease; diammonium glycyrrhizinate; liver protection

1. Introduction

The liver is an important organ of human metabolism and the largest detoxification organ [1]. A number of studies have shown that after alcohol consumption, alcohol enters the blood after being absorbed through the gastrointestinal tract, and metabolic reactions occur in the liver. Long-term irrational eating and drinking habits can cause liver damage and lead to a range of liver diseases, such as alcoholic liver disease (ALD) [2]. ALD manifests as fatty liver in the early stage, which can then develop into alcoholic hepatitis, liver fibrosis, cirrhosis, and even liver failure [3]. ALD is the main cause of morbidity and mortality in industrialized countries and developing countries and is an advanced disease that is difficult to cure [4]. Therefore, it is important to study the mechanism of ALD and its treatment.

Various microbes reside in the intestinal tract of animals, and the number of microbes is very large. These microbes are very closely related to the physiological activities, metabolism, and immunity of the host. Under normal conditions, the gut microbiota and the host coexist harmoniously, and gut microbiota play important roles in maintaining a normal immune system, preventing pathogenic bacteria from colonizing the body, and the digestion and absorption of nutrients. When the gut microbiota composition changes, symbiotic disorders can occur, causing various diseases [5–9]. A large number of experiments have shown that the occurrence and development of liver diseases are closely related to changes in gut microbiota. Long-term alcohol abuse can change the structure and distribution of gut microbiota in the body, causing mucosal damage and bacterial translocation, reducing the number of beneficial bacteria, increasing the number of harmful bacteria, and aggravating liver cell damage [10–12]. Studies have shown that by regulating the diversity of the gut microbiota, the composition of the gut microbiota can be optimized, an increase in beneficial bacteria can be promoted, and the growth of

pathogenic bacteria can be inhibited, thereby playing a protective role against alcoholic liver injury [13].

A large number of studies have shown that the active substances in mushrooms, such as *Hericium erinaceus* and *Ganoderma lucidum,* can be used as prebiotics to regulate gut microbes, thereby improving the health of the body [14]. *Ganoderma lucidum* spore powder (GLSP) is a type of spore ejected from the fruiting body of *G. lucidum* at the maturation stage [15,16], has all the genetic material and health care functions of *G. lucidum* [17,18], and is an extremely important medicinal and edible fungus. Modern pharmacological and clinical studies have shown that GLSP is rich in *G. lucidum* polysaccharides, triterpenes, proteins, and amino acids and is often used in the treatment of diseases, such as cancer, tumors, chronic liver diseases, insomnia, and low immunity [19–24]. GLSP is an excellent regulator of microbes and can regulate the gut microbiota and improve the immunity of the body [25]. A large number of studies have shown that GLSP can reduce cell damage, promote liver cell regeneration, and play a protective role in the liver [26]. *G. lucidum* spores can be divided into sporoderm-broken and sporoderm-unbroken spores [27]. Studies have shown that the extraction rate of bioactive components and the biological effects of *G. lucidum* spores are improved [28]. To evaluate the hepatoprotective effect and ability to regulate gut microbiota of both sporoderm-broken and sporoderm-unbroken GLSP and to identify differences between sporoderm-broken and sporoderm-unbroken GLSP, this study established a model of acute liver injury in mice caused by 50% ethanol and analyzed the liver function, anti-inflammatory indexes, changes in gut microbiota, and pathological sections from mice treated with diammonium glycyrrhizinate (DG, positive control drug), sporoderm-broken GLSP and sporoderm-unbroken GLSP to provide a theoretical basis for the clinical application of GLSP.

2. Materials and Methods

2.1 G. lucidum

Both sporoderm-broken (catalog number: 20181018) and sporoderm-unbroken (catalog number: 20181102) GLSP were purchased from Jilin Beizhi Biotechnology Co., Ltd. (Jilin, Jilin, China).

2.2 Animals

A total of 50 SPF grade C57BL/6 male mice, weighing 20 $\pm$ 2 g, were purchased from Liaoning Changsheng Biotechnology Co., Ltd. (Benxi, Liaoning, China), experimental animal use license number: SCXK Liao 2015-0001. This experiment was approved by the Ethics Committee of Changchun University of Traditional Chinese Medicine, approval number: 20190126.

2.3 Reagent

Sodium carboxymethyl cellulose (CMC) (catalog number: 9004-32-4), sodium chloride injection (catalog number: 7647-14-5), and enteric-coated DG capsules (catalog number: 79165-06-3) were purchased from Chia Tai-Tianqing Pharmaceutical Co., Ltd. (Nanjing, Jiangsu, China). Aspartate aminotransferase (AST), alanine aminotransferase (ALT) (catalog number: 9000-97-9), interleukin-18 (IL-18) (catalog number: 9000-86-6), leukocyte interleukin 1β (IL-1β) (catalog number: M9368), tumor necrosis factor α (TNF-α) (catalog number: 144796-70-3), and enzyme-linked immunosorbent assay (ELISA) kits were purchased from Shanghai Enzyme-linked Biotechnology Co., Ltd. (Shanghai, China).

2.4 Evaluation of Liver Injury Repair Ability

2.4.1 Preparation of the Test Drugs

An appropriate amount of dry sporoderm-broken and sporoderm-unbroken GLSP was added to 0.5% CMC solution and dissolved by ultrasonication for 20 min (KQ-500DA, Kunshan Ultrasound Instrument Co., Ltd., Kunshan, Jiangsu, China) to prepare a suspension with concentration of 6 mg/mL, which was stored at 4 °C for later use.

2.4.2 Animal Grouping and Drug Administration

Fifty mice were randomly divided into 5 groups, with 10 mice in each group: the control group (CG), the 50% ethanol model group (MG), the positive control group treated with DG (DGG), the sporoderm-broken GLSP group (BG), and the sporoderm-unbroken GLSP group (UG). After 5 days of adaptive feeding, the CG and MG were given an equal volume of 0.5% CMC solution for 10 days; the DGG, BG, and UG were administered drug at 0.2 mL/10 g according to mouse body weight for 10 days; and mouse body weight was recorded daily. On the 9th day, at 2 h after drug administration, except for the CG, the mice in the other 4 groups were intragastrically administered 50% ethanol at 10 mL/kg twice at an interval of 12 h. The CG was given an equal dose of water. Twelve hours later, the mice were subjected to orbital blood collection and sacrificed by cervical dislocation. Liver and stomach tissues were dissected, washed, and stored in a –80 °C freezer for further analysis. After sacrifice, feces in the bowels of mice were collected into a sterile centrifuge tube, which was immediately placed in liquid nitrogen for quick freezing for the detection of gut microbiota. During the study, diet and water were not restricted, and the bedding was changed daily. The detailed experimental protocol and drug administration are shown in Fig. 1.

2.4.3 Detection of Liver Function and Inflammatory Factors in Mice

Whole blood was centrifuged at 5000 r/min for 10 min, and the serum was collected to detect the levels of AST and ALT 10% liver homogenate was prepared with

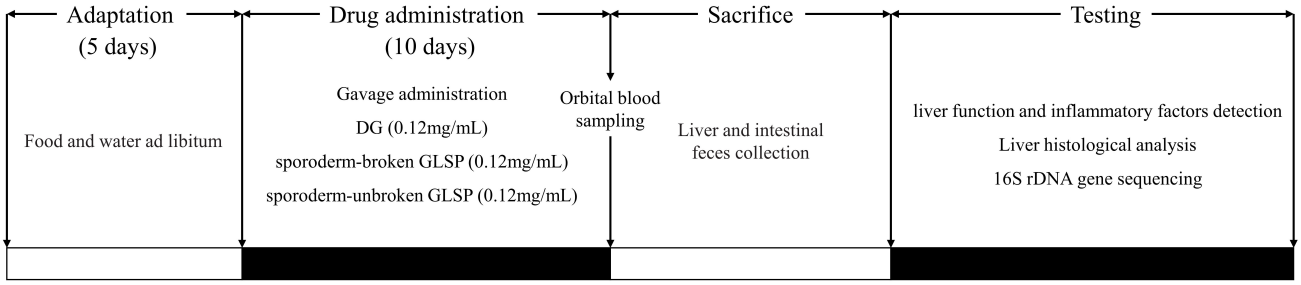

Fig. 1. The experimental protocol and drug administration.

0.1 g of liver tissue and 0.9 mL of saline and centrifuged (TGL-16M, Hunan Kaida Scientific Instruments Co., Ltd., Changsha, Hunan, China), and the supernatant was taken for determination of IL-1β, IL-18, and TNF-α levels. All operations followed the kit instructions.

2.4.4 Liver Histological Analysis

Liver tissues from the same part of the liver in each group were fixed with 10% formaldehyde solution. The liver tissues were dehydrated, cleared, embedded in paraffin, sectioned, and stained with hematoxylin-eosin (HE), and histopathological changes in the liver were observed at 200$\times$ magnification under a microscope.

2.4.5 16S rDNA Gene Sequencing

Fecal samples from 8 mice in each group were randomly selected and sent to Shanghai Genesky Bio-Tech Co., Ltd. (Shanghai, China) for polymerase chain reaction (PCR) amplicon sequencing. The integrity and quality of genomic DNA were examined using agarose gel electrophoresis (DYCP-31DN, Beijing Liuyi Biotechnology Co., Ltd., Beijing, China) and a Nanodrop 2000 spectrophotometer (NanoDrop 2000, Thermo Fisher Scientific, Waltham, MA, USA). Qualified samples with clearly visible electrophoretic bands and no significant degradation were selected for high-fidelity PCR amplification. Sequencing was performed using the MiSeq platform, followed by bioinformatics analysis. TrimGalore, FLASH2, mothur, and usearch software were used to remove unusable sequences, and the resulting paired sequences were spliced to identify and remove primers. Finally, optimized sequences with high quality and reliability were obtained. Sample Shannon curves, rank abundance distribution curves and species accumulation curves were plotted to determine species abundance and species evenness. Next, α-diversity indices, including Observed, Abundance- and Incidence-based Coverage Estimators (ACE), Chao, Shannon, Simpson, and Coverage, were calculated to obtain the species richness and diversity. β-diversity was also analyzed to show the similarity of intestinal bacterial composition between samples. Results were visualized using principal component analysis (PCA), principal coordinate analysis (PCoA), and non-metric multidimensional scaling (NMDS). To further understand the gut microbiota composition, sequences with a similarity greater than 97% were grouped into the same operational taxonomic unit (OTU), and the microbiota composition was statistically analyzed at the levels of kingdom, phylum, class, order, family, genus, and species. In this analysis, the Kruskal-Wallis (KW) rank sum test was used to assess the differential abundance between the groups. In addition, linear discriminant analysis effect sizes (LEfSe) were applied to determine the microbial groups that best represented the characteristics of each group. Then, linear discriminant analysis (LDA) was used to estimate the effect of the abundance of each microorganism on the different effects. Taxa with higher LDA scores indicated higher agreement; taxa with LDA scores >2 and $p < 0.05$ were considered significant. In addition, a phylogenetic investigation of the community by reconstructing the unobserved state (PICRUst) was used to predict the functional enrichment of different microorganisms.

2.4.6 Data Processing

Experimental results are expressed as the mean $\pm$ standard deviation (SD). Differences between groups were analyzed using one-way analysis of variance (ANOVA) in IBM SPSS 22.0 (IBM Corp., Chicago, IL, USA). $p < 0.05$ indicated a significant statistical difference. Figures were plotted using GraphPad Prism 5.0 (GraphPad Software Inc., La Jolla, CA, USA).

3. Results

3.1 Improvement Effect of GLSP on Acute Alcoholic Liver Injury

AST and ALT levels in mouse serum are shown in Fig. 2. Compared with levels in the CG, the serum AST and ALT levels in the mice in the MG were significantly increased ($p < 0.0001$), indicating that the liver had been damaged. Compared with the MG, the DGG and BG showed significantly reduced levels of AST and ALT in the serum ($p < 0.0001$), while the UG showed significantly reduced ALT levels ($p = 0.0002$), but the reduction in serum AST levels was not significant.

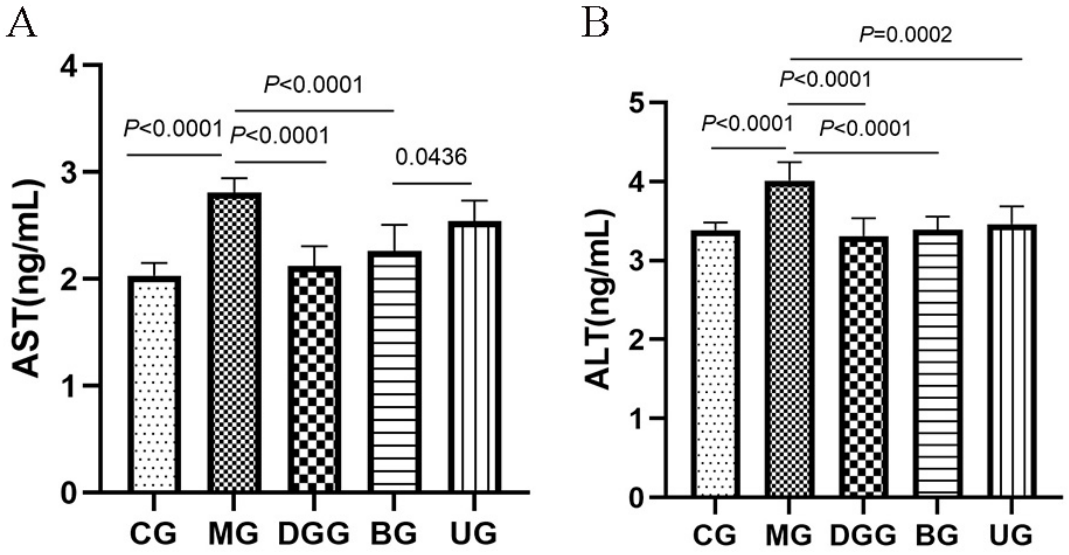

Fig. 2. GLSP treatment affected the serum levels of (A) AST and (B) ALT in mice.

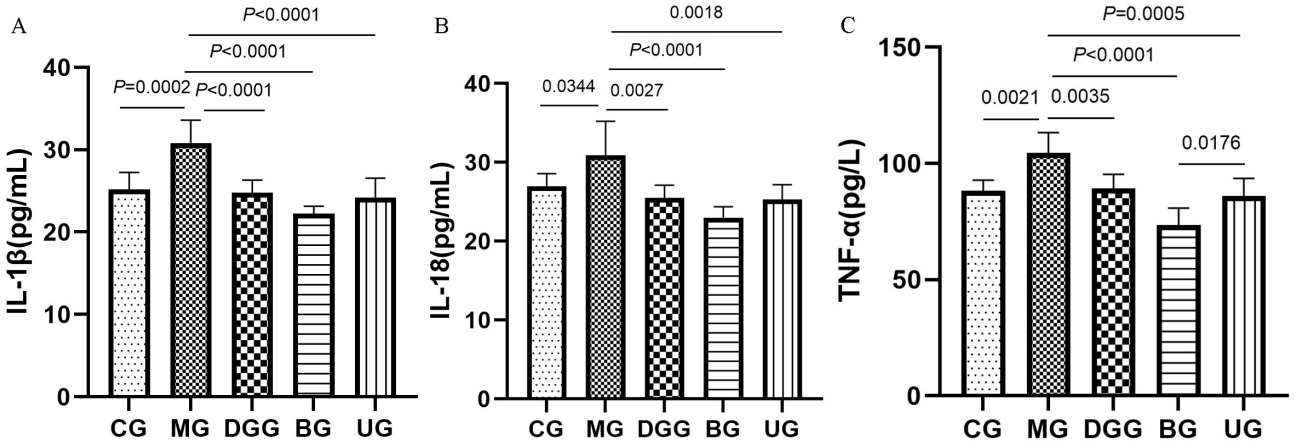

Fig. 3. FLPs treatment regulated the levels of the (A) IL-1β, (B) IL-18 and (C) TNF-α in the liver of mice.

3.2 Effect of GLSP on Inflammatory Factors in the Livers of Mice

Fig. 3 shows that IL-1β, IL-18, and TNF-α levels in the livers of mice in the MG were significantly increased compared with levels in the CG, among them, the increase in IL-1β was particularly significant (p = 0.0002); compared with levels in the MG, IL-1β, IL-18, and TNF-α levels were reduced in the livers of mice in the DGG, BG, and UG, and the treatment effect was more significant in the BG ($p < 0.0001$).

3.3 Liver Pathology Results

HE-stained sections of liver tissues were observed under an optical microscope (Fig. 4), each group has two parallel liver histopathology sections. As shown in the figure, in the CG, the morphology of the liver cells was normal, the structure of the liver lobules was clear, the hepatic cords were neatly arranged, the liver sinusoids were not significantly dilated or squeezed, no swelling or inflammation was evident, and many hepatocytes with loose cytoplasm were observed, which may have been caused by glycogen-induced lysis. In the MG, edema to balloon-like degeneration, cytoplasmic vacuolization, and more common central vein and portal vein congestion and expansion were noted, and large areas of bleeding (yellow arrow) and white blood cells (blue arrow) were observed. In the GLSP-treated groups, no significant pathological changes were observed in liver cells, and hepatocytes were morphologically intact and well arranged, with more hepatocytes having loose cytoplasm and tending to exhibit a normal structure.

3.4 Analysis of Intestinal Microbial Diversity in Mice

Forty samples were sequenced to provide 15,501,589 raw sequences. The average sequence length was in the range of 400–500 bp, which matched with the sequence length of the 16S rDNA V3–V4 region. Therefore, the subsequent analysis was expected to provide reliable results. The Rank-abundance curve (Fig. 5A) can explain the

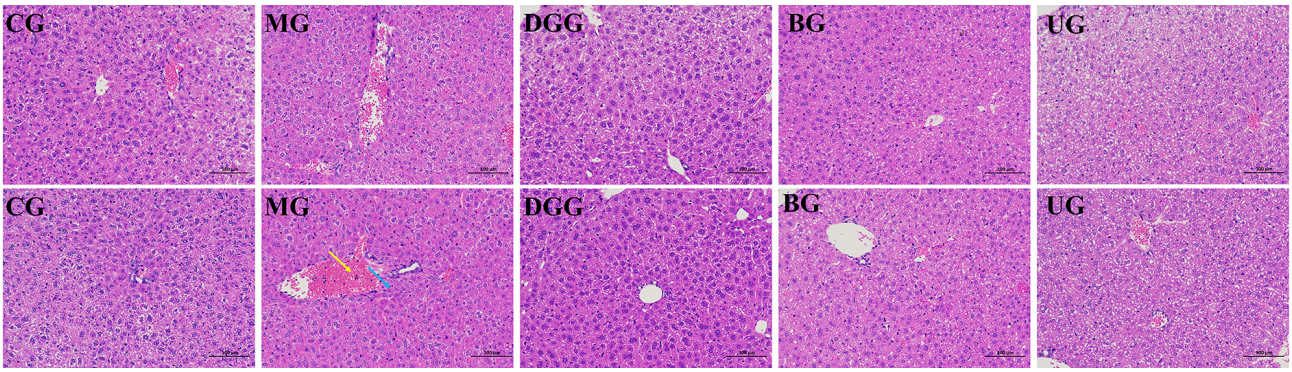

Fig. 4. Pathological sections of liver tissues (H&E staining ×200).

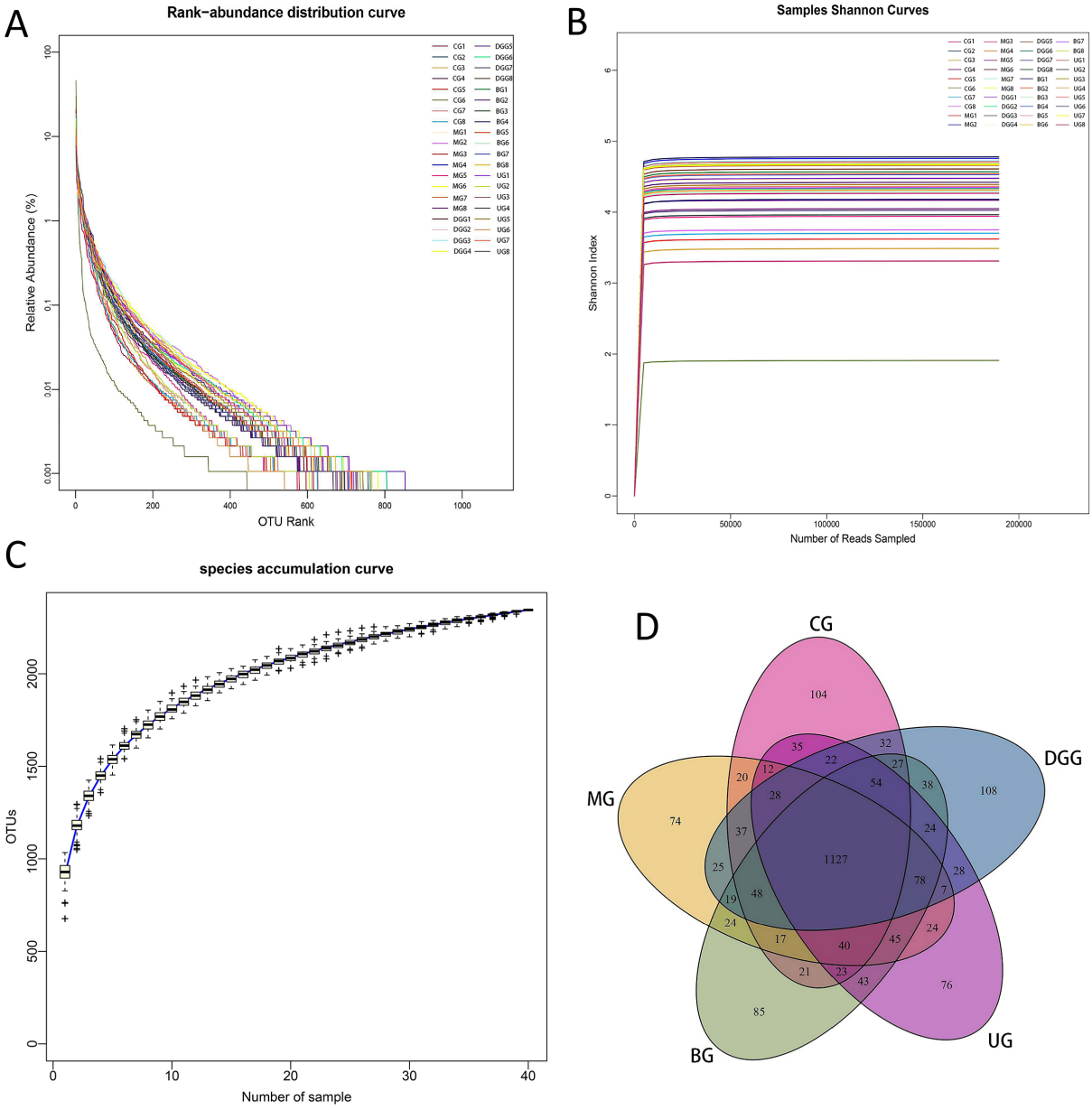

Fig. 5. 16S rDNA analysis of key operational taxonomic units (OTUs) of gut microbiota in mice. (A) Rank-abundance distribution curve. (B) Samples Shannon curves. (C) Quality analysis of sequencing result. (D) Venn diagram.

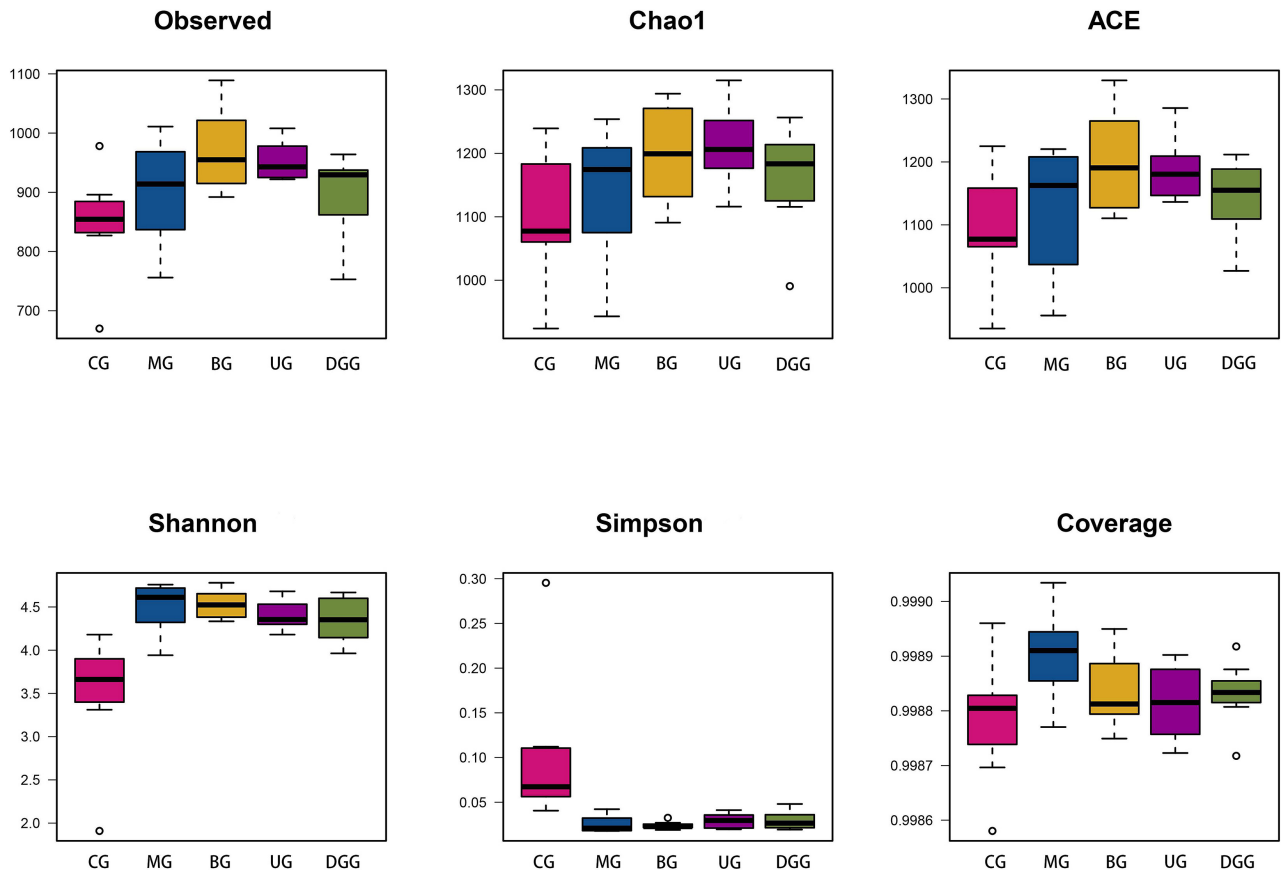

Fig. 6. α**-diversity analysis of gut microbial community structure in each group.**

species richness and community uniformity. In this study, all groups showed a large and gently decreasing range on the horizontal axis, indicating a high species richness and uniform species distribution of intestinal flora in mice in each treatment group. The Shannon curve (Fig. 5B) reflects the microbial community diversity, and its value is positively correlated with the community diversity. In this study, the curves of all groups tended to be flat, indicating that the amount of data met the sequencing requirements, and thus, the data comprehensively reflected the microbial diversity of the samples. Species accumulation curves (Fig. 5C) are used to depict the increase of species with increasing sampling size, and is widely used to determine the adequacy of sampling size. It is widely used to determine the adequacy of the sample size. The curve flattens out with the increase in the number of samples measured, indicating that the species in this environment do not increase significantly with the increase in the sample size and that the sampling size is adequate.

After clustering the gene sequences of mouse intestinal bacteria from each sample, which were obtained by high-throughput sequencing, they were grouped into different OTUs based on the similarity between sequences. The clustering and bioinformatics of OTUs were performed at a 97% similarity level, and a total of 2345 OTUs were obtained (Fig. 5D). The total number of OTUs shared by the 5 treatment groups was 1127. The number of OTUs specific to the MG was lower than that specific to the CG, while the number of OTUs specific to the BG was significantly higher than that specific to the MG and the UG. This finding indicates that different treatments can significantly affect the intestinal flora of mice.

The α-diversity indices of mouse intestinal flora under different treatments are shown in Fig. 6. The Observed index indicates the sum of the number of species with an abundance greater than 0 in the community; the Chao1 index and ACE index are used to reflect the abundance of the community; the Shannon index and Simpson index are used to evaluate the diversity of the community; the Coverage index reflects the coverage of the flora. The Observed index, Chao1 index, ACE index and Shannon index of the intestinal community were higher in the BG and UG mice than in CG mice, with the descending order BG $>$UG $>$CG. The results showed that treatment with GLSP can increase the gut microbe population size and community diversity in mice. This result indicates that GLSP treatment significantly increased the population number and the community diversity level of mouse intestinal flora, and the BG showed a more significant difference in the population number and diversity.

β-Diversity analysis was performed to investigate the similarity in the structure and composition of the gut mi-

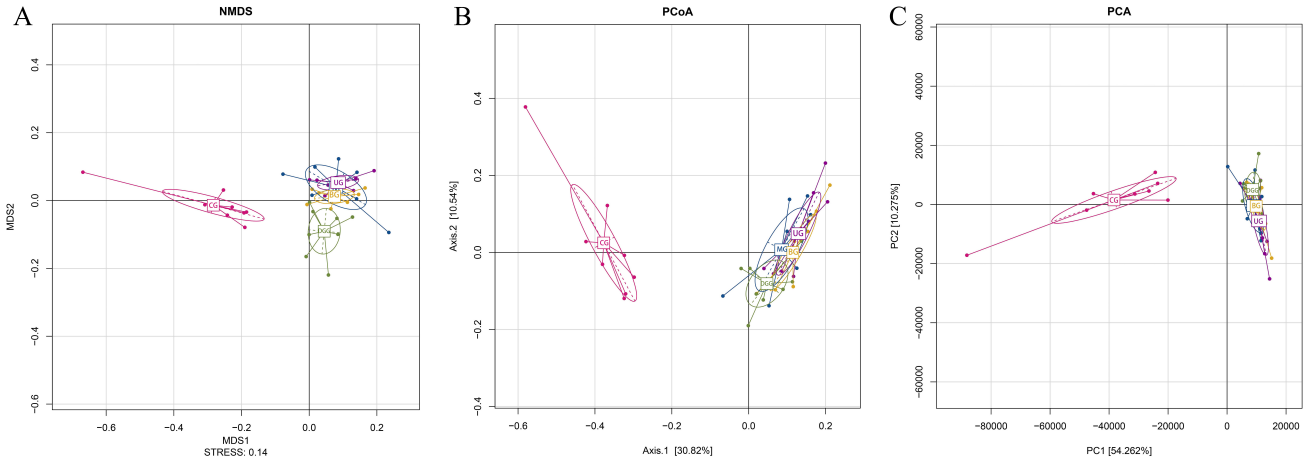

Fig. 7. β-diversity analysis of gut microbial community structure in each group. (A) PCA. (B) PCoA. (C) NMDS.

crobial community in different stool samples or groups (Fig. 7A–C). The results showed that the microbial community structure in the CG was significantly different from that in the MG, while the community structure in the BG and UG was not significantly different from that in the MG. This finding indicates that the effect of GLSP treatment on the intestinal microbial community structure in mice with acute alcoholic liver injury was not significant.

3.5 Analysis of the Structure of the Mouse Gut Microbiota

To visually observe the consistency of the species composition in each group and differences in the species composition between groups, species with a relative abundance >1% were selected to draw histograms at the phylum and genus levels (Fig. 8A and Fig. 9A). Species and samples were clustered based on distance. The similarity between species or the distance between samples on the clustering tree reflect similarities and differences in the species compositions of all samples at a given taxonomic level, and the top 100 species with the highest abundance in the samples were selected to construct a heatmap (Fig. 9B).

Fig. 8A,C show that at the phylum level, the dominant phyla of the mouse gut microbiota were *Bacteroidetes*, *Firmicutes*, *Proteobacteria*, *Actinobacteria*, and *Verrucomicrobia*, with *Bacteroidetes* and *Firmicutes* representing more than 90% of the microbiota. Compared with levels in the CG, the relative abundance levels of *Firmicutes* (p = 0.0073) and *Actinobacteria* ($p < 0.0001$) were significantly decreased, the relative abundance levels of *Proteobacteria* (p = 0.013) was significantly increased, and the levels of *Bacteroidetes* and *Candidatus_Saccharibacteria* were slightly increased in the feces of the MG. Compared with the MG, the relative abundance of *Bacteroidetes* was increased and the relative abundance levels of *Proteobacteria* and *Candidatus_Saccharibacteria* were decreased in the feces of the DGG; the relative abundance of *Bacteroidetes* were increased, the level of *Verrucomicrobia* was decreased in the BG, and the relative abundance levels of *Proteobacteria* and *Candidatus_Saccharibacteria* were decreased in the BG; the relative abundance of *Bacteroidetes* was increased, and the relative abundance of *Proteobacteria* was decreased in the UG, but the effect was not significant. Analysis of the heatmap of the gut microbiota at the phylum level (Fig. 8B) showed that the abundance of gut microbes in the BG was increased, and the clustering of phyla in the BG and the DGG was the closest, indicating that sporoderm-broken GLSP is more effective in regulating alcohol-induced phylum-level changes in gut microbes.

Fig. 9A,C show that the relative abundance of *Lactobacillus* was significantly reduced compared with that in the CG ($p < 0.0001$), and the relative abundance levels of *Alloprevotella*, *Bacteroides*, *Helicobacter*, *Eisenbergiella*, *Escherichia_Shigella*, *Paraprevotella* and *Parabacteroides* were all increased to varying degrees in the MG. Compared with the MG, the relative abundance levels of *Escherichia_Shigella* (p = 0.0462) was significantly reduced in the BG, and the relative abundance levels of *Helicobacter* and *Eisenbergiella* were reduced in the UG, but the effect was not significant. According to the cluster analysis (Fig. 9B), the clustering of genera in the DGG and BG was the most similar, but the clustering of genera in the DGG was closer to that in the CG, indicating that GLSP may regulate alcohol-induced genus-level changes in gut microbes and that the regulatory effect of sporoderm-broken GLSP is better.

In addition, LEfSe analysis was performed on these five groups of mice for the simultaneous identification of specific taxa across phylum, class, order, family and genus levels. The histogram of LDA effect values for biomarker species is shown in **Supplementary Fig. 1**. It was found that there were 65 significantly different species in CG (LDA >2, $p < 0.05$) , and the three most different species were f_*Lactobacillaceae*, g_*Lactobacillus*, o_*Lactobacillales*; the enriched species in MG were mainly c_*Clostridia*, o_*Clostridiales* and f_*Ruminococcaceae*; differential bacteria in BG were

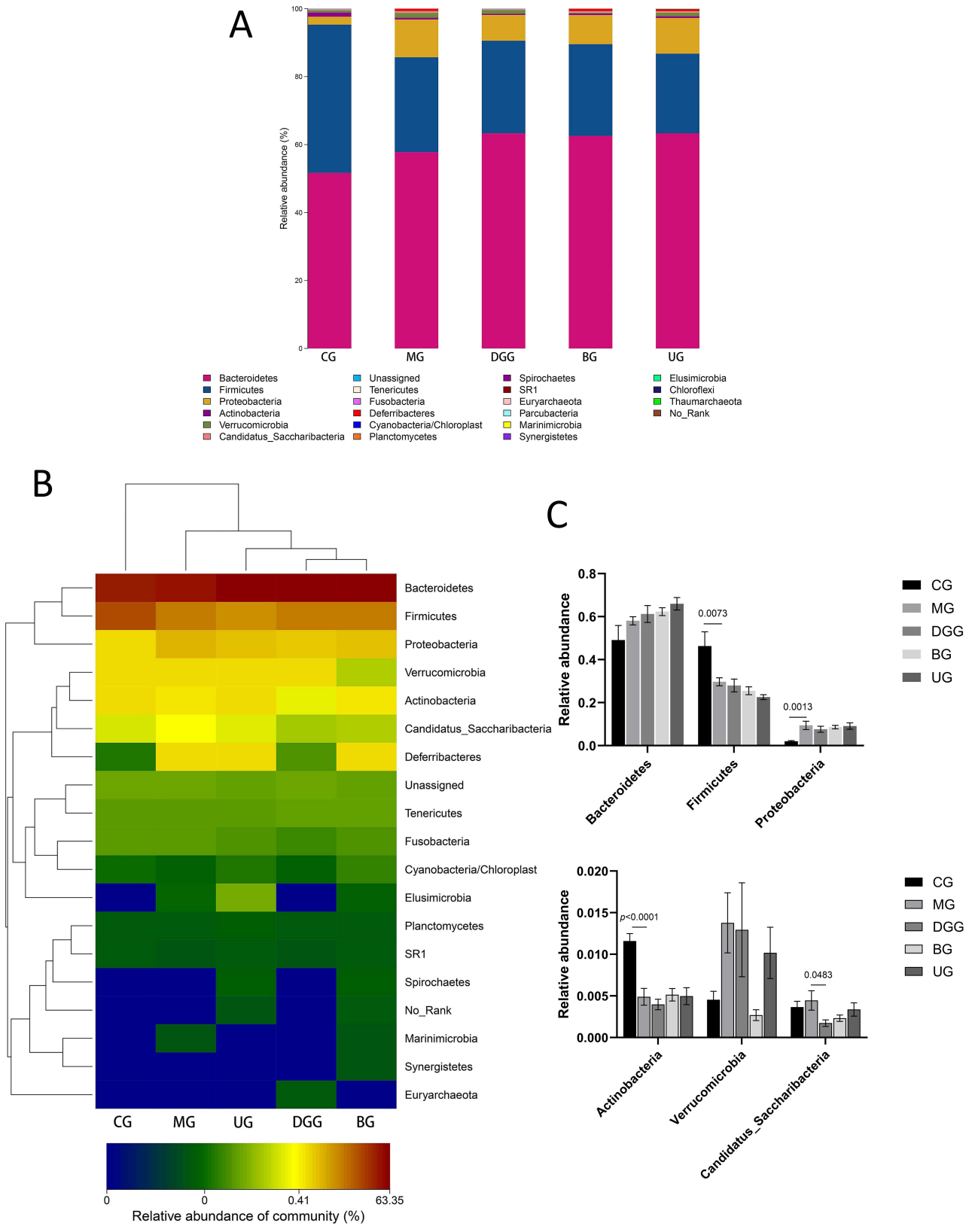

Fig. 8. Effect of GLSP on phylum-level gut microbiota in mice. (A) phylum-level histogram. (B) Cluster heatmap of species abundance. (C) Quantitative statistics of bacteria with phylum-level differences.

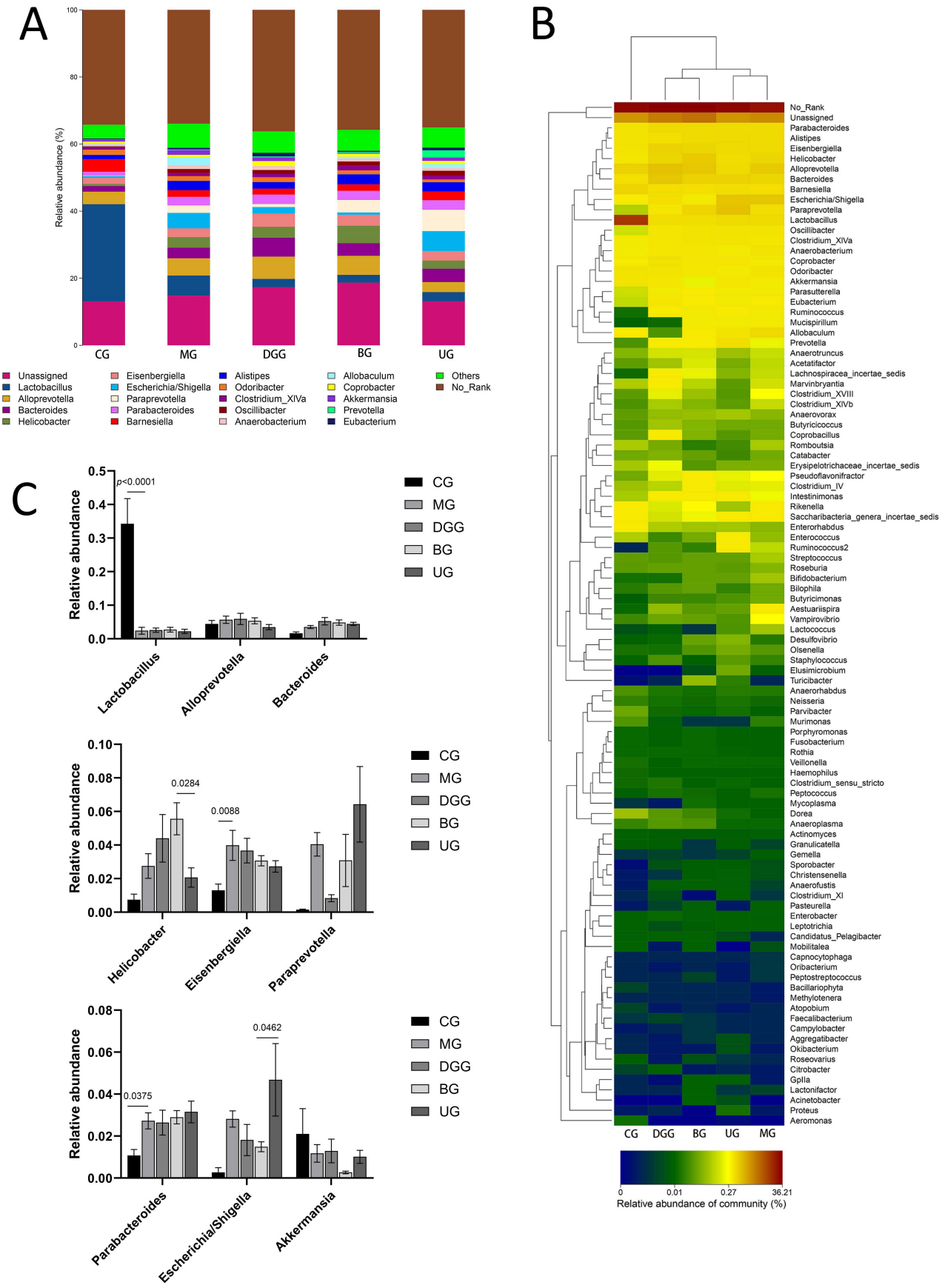

Fig. 9. Effect of GLSP on the genus-level gut microbiota in mice. (A) Genus-level histogram. (B) Cluster heatmap of species abundance. (C) Quantitative statistics of bacteria with genus-level differences.

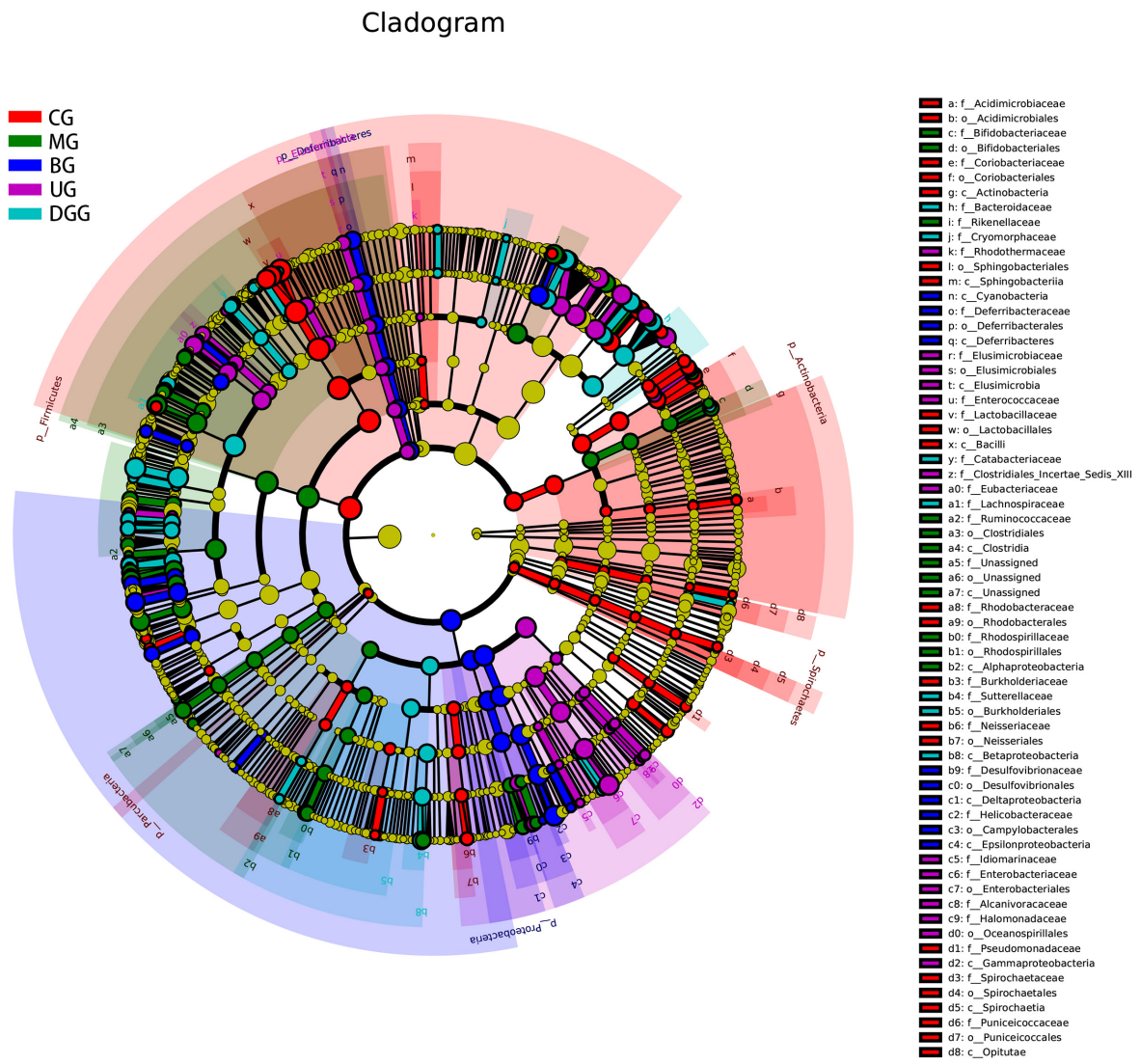

Fig. 10. Linear discriminant analysis effect size cladogram for the comparisons of the five study groups.

dominated by p_*Proteobacteria*, c_*Epsilonproteobacteria*, o_*Campylobacterales*; differential bacteria in UG were dominated by s_*uncultured_bacterium*, g_*Paraprevotella*, c_*Gammaproteobacteria*. The cladogram (Fig. 10) with different color nodes indicates microbial taxa that are significantly enriched in the corresponding groups and have a significant effect on the differences between groups. The cladogram showed that the dominant microorganisms in each group of mice were located in different phylum. p_*Firmicutes*, p_*Actinobacteria*, p_*Spirochaetes* and p_*Parcubacteria* were the most abundant dominant microorganisms in CG; p_*Deferribacteres*, p_*Proteobacteria* were the most abundant dominant microorganisms in BG; p_*Elusimicrobia* were the most abundant dominant microorganisms in UG.

Fig. 11 shows the analysis of differences in clusters of orthologous groups (COG) composition, listing the functional categories in which COG composition differed significantly between groups and the proportion in each group, with the proportion of differences and confidence intervals and *p*-values given on the right. Nucleotide transport and metabolism ($p = 0.01$), translation, ribosomal structure and biogenesis ($p = 0.014$), and lipid transport and metabolism ($p = 0.015$) were significantly downregulated in the MG mice intestinal flora compared to CG. Significant upregulation of coenzyme transport and metabolism ($p = 0.01$), translation, ribosome structure and biogenesis ($p = 0.014$), cell wall/membrane/envelope biogenesis ($p = 0.02$), and post-translational modifications, protein turnover and chaperones ($p = 0.023$) in BG mice intestinal flora compared to MG. The functions of lipid transport and metabolism ($p = 0.017$), coenzyme transport and metabolism ($p = 0.024$), and cell wall/membrane/envelope biogenesis ($p = 0.026$) were significantly upregulated in the intestinal flora of UG mice.

The kyoto encyclopedia of genes and genomes (KEGG) database is a large knowledge base for systematic analysis of gene functions, linking genomic information

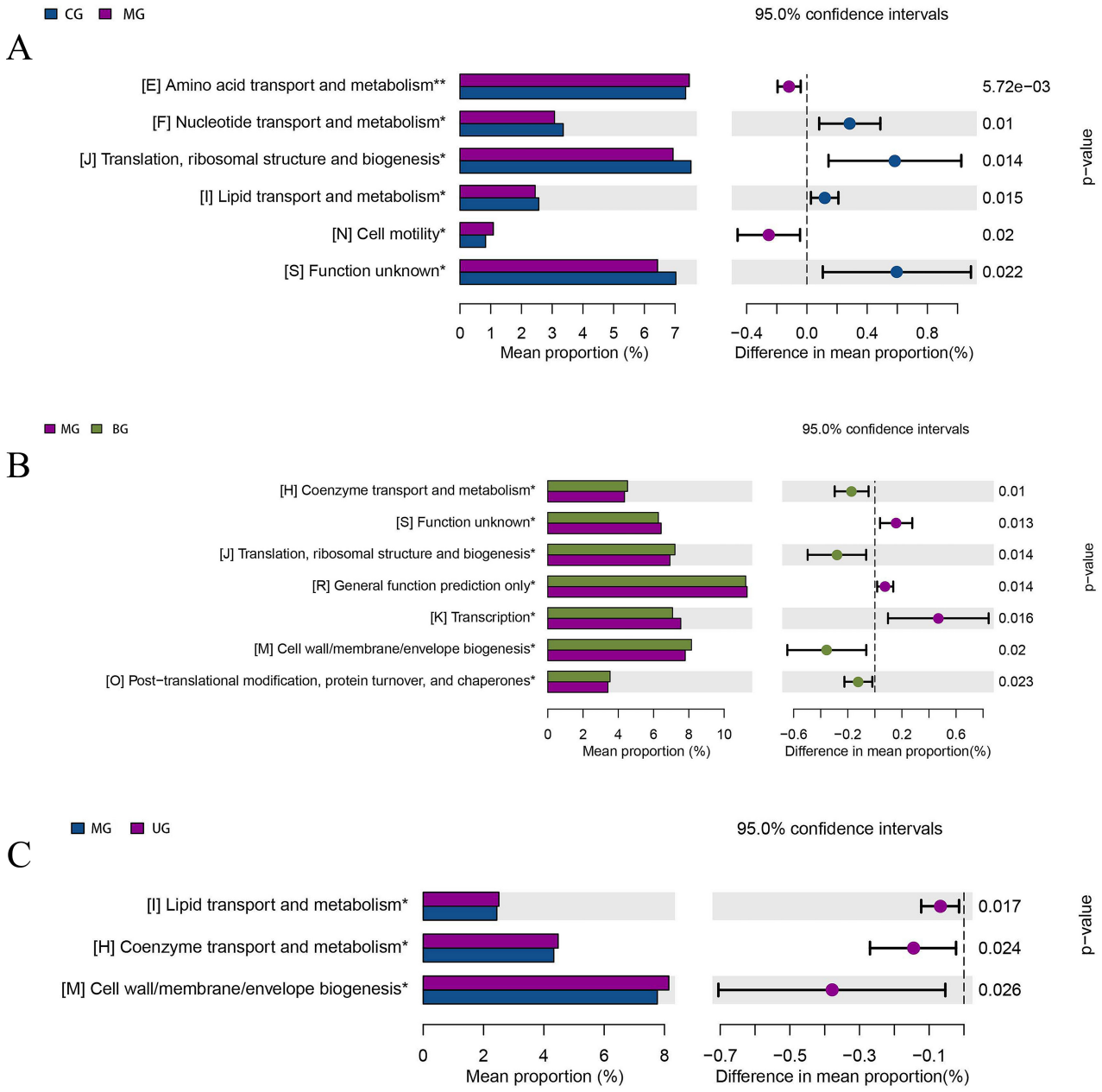

Fig. 11. COG function enrichment analysis of gut microbiota of mice. (A) CG versus MG. (B) MG versus BG. (C) MG versus UG.

and functional information. As shown in Fig. 12, the levels of 65 functions such as vibrio cholerae pathogenic cycle (p = 0.0005), bacterial motility proteins (p = 0.0007), and bacterial chemotaxis (p = 0.0011) were significantly downregulated in the intestinal flora of MG mice compared with CG; compared with MG, the levels of 25 functions such as biotin metabolism (p = 0.0041), restriction enzyme (p = 0.015), carbon fixation pathways in prokaryotes (p = 0.017) were significantly upregulated in BG mice intestinal flora, and the levels of 30 functions such as biotin metabolism (p = 0.0099), carbon fixation pathways in prokaryotes (p = 0.013) and peroxisome (p = 0.015) were significantly upregulated in UG mice.

4. Discussion

In an experimental model of acute alcoholic liver injury, this study demonstrated that GLSP may play a beneficial role in protecting the liver by regulating the gut microbial community structure.

In the normal environment of the body, AST and ALT are present in small amounts in liver cells. When cells are damaged, cell membrane permeability is enhanced, a large amount of AST and ALT are released into the blood, and their concentrations in serum are increased. Therefore, AST and ALT are often used as important indicators for the diagnosis of viral hepatitis and toxic hepatitis [29–31]. In this study, the BG showed significantly reduced serum AST and ALT levels caused by alcohol, but the UG showed a sig-

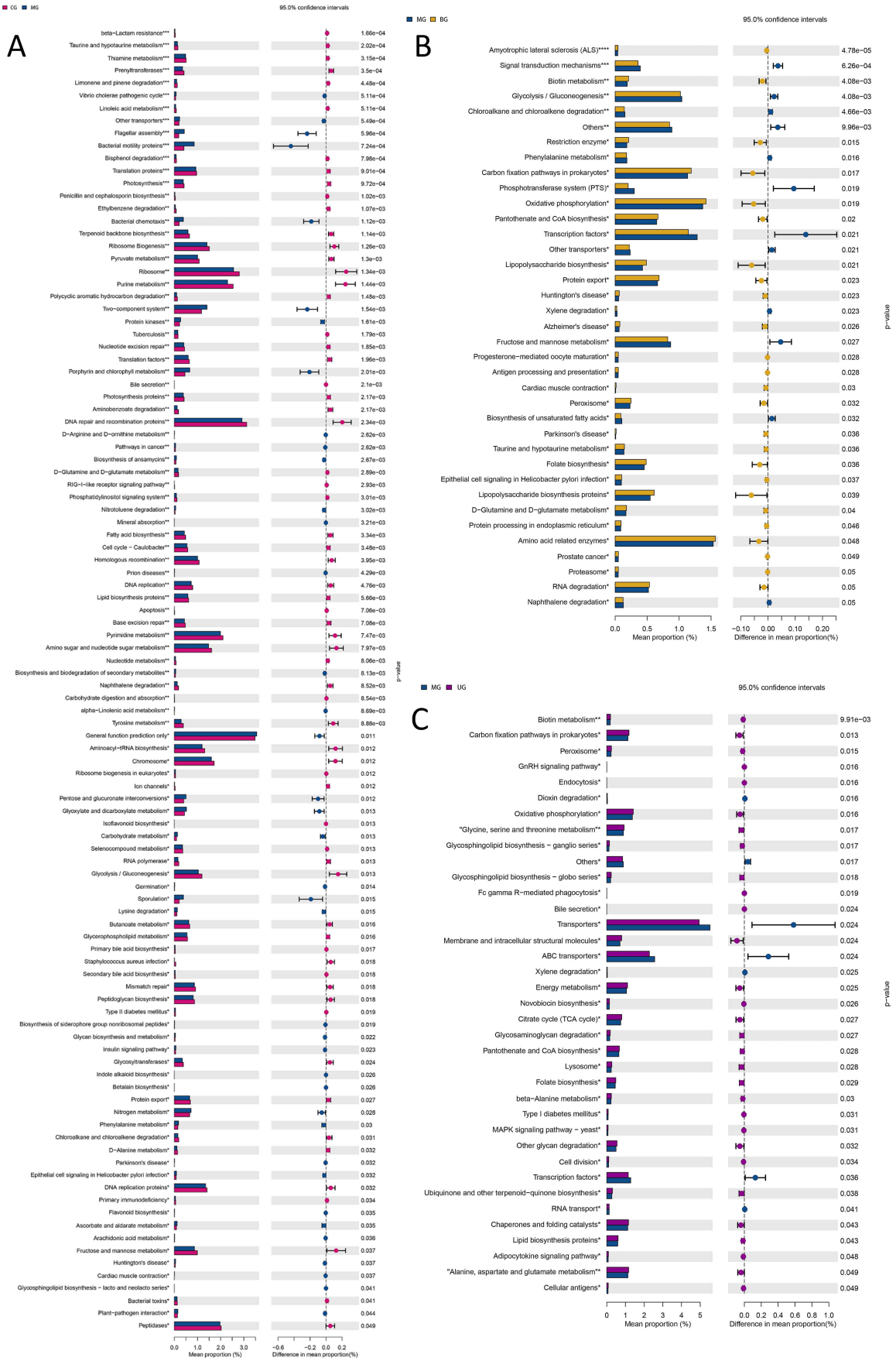

Fig. 12. KEGG function enrichment analysis of gut microbiota of mice. (A) CG versus MG. (B) MG versus BG. (C) MG versus UG.

nificant inhibitory effect only on the increased ALT level caused by liver injury and no significant effect on AST, indicating that in the BG and UG, the changes in AST and ALT levels caused by alcohol-induced liver injury were regulated, with a better effect in the BG.

Long-term intake of alcohol can lead to a sudden increase in microbial products, such as endotoxin in the blood, and the phagocytic cells located on the inner surface of liver sinusoids, such as Kupffer cells, bind to endotoxin and are activated; thus, a large number of cytokines and inflammatory mediators, such as IL-1β, IL-18, and TNF-α, are released into the body, causing hepatocyte necrosis or apoptosis [32–34]. IL-18 can induce the production of interferon (IFN)-γ and TNF-α and aggravate liver injury [35]. IL-1β can participate in the activation of immune cells, promote inflammatory cell aggregation, and induce inflammatory responses [36]. TNF-α has a variety of biological activities and can regulate the production of other inflammatory factors and induce inflammation in the liver [37]. Compared with the MG, the DGG, BG, and UG all showed reduced IL-1β, IL-18, and TNF-α levels in the liver, and the treatment effect was more significant in the BG. In summary, both sporoderm-broken and sporoderm-unbroken GLSP can reduce the secretion of TNF-α, reduce the levels of IL-1β and IL-18, and have a protective effect on the liver. Sporoderm-broken GLSP has a better effect. Comparison of liver sections from each group showed that GLSP improved the pathological changes in the liver caused by alcohol. The number of hepatocytes with vacuolar degeneration in the BG was lower than that in the UG, indicating that the therapeutic effect of sporoderm-broken GLSP was better than that of sporoderm-unbroken GLSP.

To investigate the effect of GLSP treatment on the intestinal flora of mice with acute alcoholic liver injury, 16S rDNA gene sequencing was performed on the colonic feces of mice in each treatment group. The diversity analysis of intestinal flora of mice revealed that sporoderm-broken GLSP could significantly improve the abundance and diversity of intestinal microorganisms in liver-injured mice. A number of studies have shown that long-term alcohol stress can change the intestinal permeability in the body, thereby increasing the number of *Bacteroidetes* and *Verrucomicrobia* in the cecum and reducing the growth of bacteria with anti-inflammatory activity, such as *Firmicutes* [38]. *Bacteroidetes* is the second most dominant phylum in the intestine, participates in the metabolism of carbohydrates and lipids in the intestine, and has a very important impact on the health of the host [39]. *Firmicutes* can participate in carbohydrate metabolism and maintain healthy gut microbiota [40]. The relative abundance ratio of *Bacteroidetes* to *Firmicutes* is an important indicator of changes in microbiota composition, and changes in this indicator may lead to the occurrence of complications, such as obesity, diabetes, inflammatory bowel disease, and liver disease [41–44]. Studies have shown that *G. lucidum* polysaccharides can reverse *Bacteroidetes*/*Firmicutes* levels, increase anti-inflammatory bacteria and short-chain fatty acid-producing bacteria, reduce some disease-related bacteria, and remodel the gut microbiota [45]. In this study, compared with levels in the CG, the *Bacteroidetes*/*Firmicutes* levels in the MG were significantly increased, indicating that alcohol caused an imbalance in the gut microbiota in mice and that the model was established successfully. Compared with the MG, the *Bacteroidetes*/*Firmicutes* levels in the DGG, BG, and UG did not show significant changes, indicating that GLSP and the positive control drug did not alleviate alcoholic liver injury by reversing the *Bacteroidetes*/*Firmicutes* levels. Compared with that in the CG, the level of *Lactobacillus* in the MG was significantly reduced, which is consistent with the results of Hartmann *et al*. [46], indicating that the occurrence of ALD may be related to a decrease in the relative abundance of *Lactobacillus*. Studies have shown that the *Proteobacteria* level in the intestines of most diseased hosts is higher than that in healthy hosts, and a large amount of proinflammatory factors are released, which increases intestinal permeability, destroys the redox balance in the intestine, causes endotoxin leakage into the plasma, and eventually causes liver steatosis, inflammation, and apoptosis [47–50]. *Escherichia_Shigella* can adversely affect liver lipid metabolism [51]. Zhao *et al*. [52] found that increases in the relative abundance levels of *Proteobacteria* and *Escherichia_Shigella* in the intestine of rats can cause liver damage. In the present study, compared with levels in the CG, the relative abundance levels of *Proteobacteria* and *Escherichia_Shigella* in the MG were increased. Compared with levels in the MG, the relative abundance levels of *Proteobacteria* and *Escherichia_Shigella* in the DGG and BG showed a decreasing trend, the inhibitory effect on *Escherichia_Shigella* in the BG was better than that in the DGG, and the level of *Escherichia_Shigella* in the BG was close to the normal level in the CG, indicating that the sporoderm-broken GLSP alleviated the alcohol-induced increases in *Proteobacteria* and *Escherichia_Shigella* levels in the intestine, thereby achieving a liver-protecting effect. Evidence indicates that the relative abundance of *Candidatus_Saccharibacteria* in the intestines of alcohol-treated mice may increase [53–55]. *Candidatus_Saccharibacteria* invades the human skin, mucous membranes, and internal organs, resulting in a variety of acute and chronic diseases, such as interdigital erosion, rash, thrush, intracardiac encephalitis, and meningitis [56]. In the present study, compared with the CG, the *Candidatus_Saccharibacteria* level in the MG was increased but not significantly, and after BG treatment, the relative abundance of *Candidatus_Saccharibacteria* decreased to the normal level, which may be another means to protect the liver. Analysis of the phylum- and genus-level heatmaps of the gut microbiota of mice in each group showed that sporoderm-broken GLSP increased abundance levels in the mice in the liver injury model, and the cluster analysis of the

microbiota showed that the regulatory effect of sporoderm-broken GLSP on the genus-level gut microbiota was most similar to that of the positive control drug. In addition, the functions of the identified microbiota were predicted, and the levels of functions such as translation, ribosome structure and biogenesis, and lipid transport and metabolism were found to be down-regulated in the intestinal flora of mice with acute liver injury, and GLSP treatment upregulated the levels of these functions; therefore, we speculate that these functions may also play an important role in the development of acute alcohol liver injury. In summary, alcohol consumption can significantly change the gut microbial abundance and diversity, but sporoderm-broken GLSP can partially regulate these changes and effectively ameliorate alcoholic liver injury.

5. Conclusions

This study investigated the ability of both sporoderm-broken and sporoderm-unbroken GLSP to mitigate alcoholic liver injury in mice. The results showed that GLSP reduced the increased AST and ALT levels in the blood caused by liver injury; decreased the release of inflammatory factors, including IL-1β, IL-18, and TNF-α; improved damaged liver cells; regulated the gut microbial community diversity; increased the relative abundance levels of beneficial bacteria and reduced the reproduction of harmful bacteria. The results of the various experiments in this study showed that the ability of sporoderm-broken GLSP to heal alcoholic liver injury in mice was greater than that of sporoderm-unbroken GLSP. And GLSP can also regulate the function of intestinal microbiota.

Availability of Data and Materials

The datasets used and analyzed during the current study are available from the corresponding author on reasonable request.

Author Contributions

HW and SW—designed the research study. FW—performed the research. YL—conducted the study and drafted the manuscript. XW, XL and YL—analyzed the data. CC—provided administrative support. All authors contributed to editorial changes in the manuscript. All authors read and approved the final manuscript.

Ethics Approval and Consent to Participate

This experiment was approved by the ethics committee of Changchun University, in accordance with the relevant provisions of the national ethics of animal use in research (approval number: 20190126).

Acknowledgment

The authors thank the Institute of Ginseng Science of Changchun University of Traditional Chinese Medicine for its support of the study.

Funding

This study was supported by Jilin Province Science and Technology Development Plan Project (No. 20210401121YY), the Training Plan for Young Scientists of "Xinglin Scholar Project" of Changchun University of traditional Chinese Medicine (QNKXJ2-2021ZR03), and Jilin Province local herbal standardization project (JLPZGF-2018-005).

Conflict of Interest

The authors declare no conflict of interest.

Supplementary Material

Supplementary material associated with this article can be found, in the online version, at https://doi.org/10.31083/j.fbl2802023.

References

[1] Wang QX, Ma X. Ten years of research progress in the field of non-viral liver disease. Chinese Journal of Hepatology. 2021; 29: 116–120. (In Chinese)

[2] Kim S, Ko I, Jin J, Hwang L, Kim B, Baek S. Study on the pathogenesis of liver injury caused by alcohol and drugs. Journal of Exercise Rehabilitation. 2021; 17: 319–323.

[3] Song X, Liu Z, Zhang J, Zhang C, Dong Y, Ren Z, *et al*. Antioxidative and hepatoprotective effects of enzymatic and acidic-hydrolysis of Pleurotus geesteranus mycelium polysaccharides on alcoholic liver diseases. Carbohydrate Polymers. 2018; 201: 75–86.

[4] Seitz HK, Neuman MG. The History of Alcoholic Liver Disease: From an Unrecognized Disease to One of the Most Frequent Diseases in Hepatology. Journal of Clinical Medicine. 2021; 10: 858.

[5] Almeida J, Galhenage S, Yu J, Kurtovic J, Riordan SM. Gut flora and bacterial translocation in chronic liver disease. World Journal of Gastroenterology. 2006; 12: 1493–1502.

[6] Bercik P, Collins SM, Verdu EF. Microbes and the gut-brain axis. Neurogastroenterology and Motility. 2012; 24: 405–413.

[7] Li B, Gong T, Hao Y, Zhou X, Cheng L. Mining the Gut Microbiota for Microbial-Based Therapeutic Strategies in Cancer Immunotherapy. Frontiers in Oncology. 2021; 11: 721249.

[8] Nguepi TIS, Song H. Mushrooms Bioactive as Prebiotics to Modulate Gut Microbiota in Relationships with Causes and Prevention of Liver Diseases (Review). International Journal of Medicinal Mushrooms. 2020; 22: 509–519.

[9] Zhang Y, Zhang Y, Si H. Lung and gut microbiota and their interaction with the carcinogenesis and development of lung cancer: a review. Chinese Journal of Biotechnology. 2021; 37: 3789–3800. (In Chinese)

[10] Park J, Kim S, Lee NY, Kim J, Jung J, Jang M, *et al*. Role of Microbiota-Derived Metabolites in Alcoholic and Non-Alcoholic Fatty Liver Diseases. International Journal of Molecular Sciences. 2021; 23: 426.

[11] Ding J, Jin Z, Yang X, Lou J, Shan W, Hu Y, *et al*. Role of gut microbiota via the gut-liver-brain axis in digestive diseases. World Journal of Gastroenterology. 2020; 26: 6141–6162.

[12] Sharma SP, Suk KT, Kim DJ. Significance of gut microbiota in alcoholic and non-alcoholic fatty liver diseases. World Journal of Gastroenterology. 2021; 27: 6161–6179.

[13] Hartmann P, Seebauer CT, Schnabl B. Alcoholic liver disease: the gut microbiome and liver cross talk. Alcoholism, Clinical and Experimental Research. 2015; 39: 763–775.
[14] Kumari K. Mushrooms as source of dietary fiber and its medicinal value: A review article. Journal of Pharmacognosy and Phytochemistry. 2020; 9: 2075–2078.
[15] Dai YC. Ganoderma lucidum. Mycosystema. 2017; 36: 4. (In Chinese)
[16] Ma YH, Shao YY, Zhang WT, Zhou Y, Zhao Y, Sun YJ. Analysis of different manifestations and causes of liquid culture of Ganoderma lucidum with three traditional Chinese medicinal herbs. Pakistan Journal of Botany. 2022; 54: 977–984.
[17] Xie CL, Yan SW, Zhang ZM, Gong WB, Zhu ZH, Zhou YJ, *et al*. Mapping the metabolic signatures of fermentation broth, mycelium, fruiting body and spores powder from Ganoderma lucidum by untargeted metabolomics. LWT-Food Science and Technology. 2020; 129: 109494.
[18] Xu J, Li P. Researches and Application of Ganoderma Spores Powder. Ganoderma and Healthy: Biology, Chemistry and Industry. 2019; 1181: 157–186.
[19] Deng Y, Ma J, Tang D, Zhang Q. Dynamic biomarkers indicate the immunological benefits provided by Ganoderma spore powder in post-operative breast and lung cancer patients. Clinical & Translational Oncology. 2021; 23: 1481–1490.
[20] Liu G, Zeng T. Sporoderm-Removed *Ganoderma lucidum* Spore Powder May Suppress the Proliferation, Migration, and Invasion of Esophageal Squamous Cell Carcinoma Cells Through PI3K/AKT/mTOR and Erk Pathway. Integrative Cancer Therapies. 2021; 20: 15347354211062157.
[21] Liu M, Chen L, Zhao J, Li S. *Ganoderma* spore powder contains little triterpenoids. Chinese Medicine. 2020; 15: 111.
[22] Qin L, Wang C, Jiang X, Song Y, Feng Y, Qin L, *et al*. Effects of spore powder of ganoderma lucidum on CaSR and apoptosis-related proteins in hippocampus tissue of epilepsy following dementia: A protocol of systematic review. Medicine. 2020; 99: e21711.
[23] Shi Y, Zheng H, Hong Z, Wang H, Wang Y, Li M, *et al*. Antitumor effects of different Ganoderma lucidum spore powder in cell- and zebrafish-based bioassays. Journal of Integrative Medicine. 2021; 19: 177–184.
[24] Zhao H, Cui S, Qin Y, Liu Y, Cui X, Hu X, *et al*. Prophylactic effects of sporoderm-removed Ganoderma lucidum spores in a rat model of streptozotocin-induced sporadic Alzheimer's disease. Journal of Ethnopharmacology. 2021; 269: 113725.
[25] Sang T, Guo C, Guo D, Wu J, Wang Y, Wang Y, *et al*. Suppression of obesity and inflammation by polysaccharide from sporoderm-broken spore of Ganoderma lucidum via gut microbiota regulation. Carbohydrate Polymers. 2021; 256: 117594.
[26] Shen S, Zhu L, Wu Z, Wang G, Ahmad Z, Chang M. Production of triterpenoid compounds from *Ganoderma lucidum* spore powder using ultrasound-assisted extraction. Preparative Biochemistry & Biotechnology. 2020; 50: 302–315.
[27] Liu X, Yuan J, Chung C, Chen X. Antitumor activity of the sporoderm-broken germinating spores of Ganoderma lucidum. Cancer Letters. 2002; 182: 155–161.
[28] Ma J, Fu Z, Ma P, Su Y, Zhang Q. Breaking and characteristics of Ganoderma lucidum spores by high speed entrifugal shearing pulverizer. Journal of Wuhan University of Technology-Mater. 2007; 22: 617–621.
[29] Barbosa AD, Mueller ES, de Moraes GHK, Umigi RT, Barreto SLD, Ferreira RM. Aspartate aminotransferase and alanine aminotransferase profile and biometry of Japanese quails liver. Revists Brasileira Zootecnia-Brazilian Journal of Animal Science. 2010; 39: 308–312.
[30] Capelli R, Kitano Y, Linhares M, Da Silva D, Golse N, Karam V, *et al*. The prognostic significance of serum aspartate transaminase and gamma-glutamyl transferase in liver deceased donors. Transplant International. 2021; 34: 2247–2256.
[31] Wai-Sun Wong V, Kao J. Letter: elevated aspartate aminotransferase and aspartate aminotransferase to alanine aminotransferase ratio predicts poor survival in hepatocellular carcinoma after resection-Authors' reply. Alimentary Pharmacology & Therapeutics. 2020; 52: 1764.
[32] Delaleu N, Bickel M. Interleukin-1 beta and interleukin-18: regulation and activity in local inflammation. Periodontology 2000. 2004; 35: 42–52.
[33] Kitade H, Kanemaki T, Sakitani K, Inoue K, Matsui Y, Kamiya T, *et al*. Regulation of energy metabolism by interleukin-1beta, but not by interleukin-6, is mediated by nitric oxide in primary cultured rat hepatocytes. Biochimica Et Biophysica Acta-Molecular Cell Research. 1996; 1311: 20–26.
[34] Qu H, Gao X, Yi JJ, Wang ZY. Review on the Protective Effects of Food-Derived Natural Compounds on Alcohol-Induced Liver Injury. Food Science. 2020; 41: 283–290. (In Chinese)
[35] Finotto S, Siebler J, Hausding M, Schipp M, Wirtz S, Klein S, *et al*. Severe hepatic injury in interleukin 18 (IL-18) transgenic mice: a key role for IL-18 in regulating hepatocyte apoptosis *in vivo*. Gut. 2004; 53: 392–400.
[36] Cha Y. Effect of Foeniculum Vulgare extract on inflammatory response in lipopolysaccharide exposed rats. Journal of Korean Medicine Rehabilitation. 2014; 23: 73–83. (In Korean)
[37] Yang X, Zheng M, Zhou M, Zhou L, Ge X, Pang N, *et al*. Lentinan Supplementation Protects the Gut-Liver Axis and Prevents Steatohepatitis: The Role of Gut Microbiota Involved. Frontiers in Nutrition. 2022; 8: 803691.
[38] Bajaj JS. Alcohol, liver disease and the gut microbiota. Nature Reviews. Gastroenterology & Hepatology. 2019; 16: 235–246.
[39] Munoz R, Teeling H, Amann R, Rosselló-Móra R. Ancestry and adaptive radiation of Bacteroidetes as assessed by comparative genomics. Systematic and Applied Microbiology. 2020; 43: 126065.
[40] Mohamed Qadir R, Assafi MS. The association between body mass index and the oral Firmicutes and Bacteroidetes profiles of healthy individuals. Malaysian Family Physician. 2021; 16: 36–43.
[41] Grigor'eva IN. Gallstone Disease, Obesity and the Firmicutes/Bacteroidetes Ratio as a Possible Biomarker of Gut Dysbiosis. Journal of Personalized Medicine. 2020; 11: 13.
[42] Jasirwan COM, Muradi A, Hasan I, Simadibrata M, Rinaldi I. Correlation of gut Firmicutes/Bacteroidetes ratio with fibrosis and steatosis stratified by body mass index in patients with non-alcoholic fatty liver disease. Bioscience of Microbiota, Food and Health. 2021; 40: 50–58.
[43] Xu X, Sun S, Liang L, Lou C, He Q, Ran M, *et al*. Role of the Aryl Hydrocarbon Receptor and Gut Microbiota-Derived Metabolites Indole-3-Acetic Acid in Sulforaphane Alleviates Hepatic Steatosis in Mice. Frontiers in Nutrition. 2021; 8: 756565.
[44] Yañez CM, Hernández AM, Sandoval AM, Domínguez MAM, Muñiz SAZ, Gómez JOG. Prevalence of Blastocystis and its association with Firmicutes/Bacteroidetes ratio in clinically healthy and metabolically ill subjects. BMC Microbiology. 2021; 21: 339.
[45] Khan I, Huang G, Li X, Leong W, Xia W, Hsiao WW. Mushroom polysaccharides from Ganoderma lucidum and Poria cocos reveal prebiotic functions. Journal of Functional Foods. 2018; 41: 191–201.
[46] Hartmann P, Chen P, Wang HJ, Wang L, McCole DF, Brandl K, *et al*. Deficiency of intestinal mucin-2 ameliorates experimental alcoholic liver disease in mice. Hepatology. 2013; 58: 108–119.
[47] Lin T, Shu C, Chen Y, Lu J, Wu T, Lai W, *et al*. Like Cures Like: Pharmacological Activity of Anti-Inflammatory Lipopolysac-

charides From Gut Microbiome. Frontiers in Pharmacology. 2020; 11: 554.
[48] Rahimlou S, Bahram M, Tedersoo L. Phylogenomics reveals the evolution of root nodulating alpha- and beta-Proteobacteria (rhizobia). Microbiological Research. 2021; 250: 126788.
[49] Su H, Wang W, Zheng G, Yin Z, Li J, Chen L, *et al*. The anti-obesity and gut microbiota modulating effects of taxifolin in C57BL/6J mice fed with a high-fat diet. Journal of the Science of Food and Agriculture. 2022; 102: 1598–1608.
[50] Vasques-Monteiro IML, Silva-Veiga FM, Miranda CS, de Andrade Gonçalves ÉCB, Daleprane JB, Souza-Mello V. A rise in Proteobacteria is an indicator of gut-liver axis-mediated nonalcoholic fatty liver disease in high-fructose-fed adult mice. Nutrition Research. 2021; 91: 26–35.
[51] Liu J. Ethanol and liver: recent insights into the mechanisms of ethanol-induced fatty liver. World Journal of Gastroenterology. 2014; 20: 14672–14685.
[52] Zhao Z, Guo Z, Yin Z, Qiu Y, Zhou B. Gut Microbiota Was Involved in the Process of Liver Injury During Intra-Abdominal Hypertension. Frontiers in Physiology. 2021; 12: 790182.
[53] Bull-Otterson L, Feng W, Kirpich I, Wang Y, Qin X, Liu Y, *et al*. Metagenomic analyses of alcohol induced pathogenic alterations in the intestinal microbiome and the effect of Lactobacillus rhamnosus GG treatment. PLoS ONE. 2013; 8: e53028.
[54] Szabo G. Gut-Liver Axis Beyond the Microbiome: How the Fungal Mycobiome Contributes to Alcoholic Liver Disease. Hepatology. 2018; 68: 2426–2428.
[55] Thomas H. Gut microbiota: Intestinal fungi fuel the inflammatory fire in alcoholic liver disease. Nature Reviews. Gastroenterology & Hepatology. 2017; 14: 385.
[56] Brim H, Taylor J, Abbas M, Vilmenay K, Daremipouran M, Varma S, *et al*. The gut microbiome in sickle cell disease: Characterization and potential implications. PLoS ONE. 2021; 16: e0255956.